at equal areas per molecule for each of these comparisons, the inherent cratic entropy difference of $R \ln 2^5$ between the racemic and enantiomeric forms should make a constant contribution to the differences in the final equilibrium states of the films.[11] How this factor affects rates of mixing in these experiments is not clear to us.

On the strength of the above experiments, the resolution of a racemic film was approached by seeding with pure crystals of either enantiomer. The racemic film was spread on 10 N H_2SO_4 from a dilute hexane solution. After the usual 20 min for solvent evaporation was allowed, the barrier drive was started, and the film was compressed to 28 dyn/cm. The dashed curve in Figure 3 shows the surface pressure decrease caused by seeding the compressed film with pure racemic crystals. After 1.5 h the surface pressure had decreased nearly to the ESP of the racemic film.

The experiment was now repeated by compressing a freshly spread racemic film, but this time crystals of pure *R*-(+) enantiomer were sprinkled on the surface. The solid curve of Figure 3 shows *the rapid decrease of surface pressure to a point well below the ESP of the racemic film* and approaching that of a pure enantiomeric film.

These results imply the deposition of *R*-(+) molecules on the added crystals, leaving a partially resolved film which was composed of predominantly *S*-(−) molecules. Equivalent results were obtained by seeding with *S*-(−) crystals which would leave predominantly an *R*-(+) film. We have already presented evidence above that the free energy of enantiomer crystals is lower compared to liquid or film states than are racemic crystals.

We have tried repeatedly to detect unseeded spontaneous resolution by leaving racemic films under compression for periods of 20 h, the present limit for maintaining reasonably constant conditions. In no case have we been able to detect a spontaneous decrease in surface pressure which could not be attributed to leaks or other artifacts.

Resolution of racemates from bulk solution by seeding with enantiomers is only possible in cases, such as the present one, where the racemic crystals are more soluble than those of the enantiomer.[5] Since this is not the usual case, out study of the present situation may have been fortuitous, or the balance of forces which govern resolution from monolayers is somewhat different from those that normally apply to bulk solution.[12] It is possible that accessibility to many metastable polymorphic states, as is common for long chain surfactants, would facilitate resolutions from monolayers under conditions less favorable to normal more compact molecules. These possibilities bear on the potential relevance of these experiments to spontaneous generation of prebiotic chiral environments.

In a control experiment where a compressed *R*-(+) film was seeded with *R*-(+) crystals, the final pressure approached the ESP for a film spread from *R*-(+) crystals, whereas seeding with *S*-(−) crystals gave a final pressure approaching the ESP of a racemic film. Seeding with stearic acid, a totally different but related surfactant, produced no change in surface pressure.

To the best of our knowledge, there is no precedent for these experiments and hence no way of judging the generality of the results. With relation to the "origin of life question", it must remain as inherently speculative but permissive evidence for one possible type of chiral environment.

Acknowledgment. This work was supported by NSF Grant CHE-7622369 and NIH Grant GM-20386. The invaluable contributions of Dr. Martin Stewart and Jean Chao for the preparation and purification of materials and of Dr. Barbara Kinzig for design of the film balance and for many helpful discussions are gratefully appreciated.

(11) A referee has pointed out that the observed difference in equilibrium surface pressure between racemate and enantiomers at 70 Å^2/molecule is almost exactly the 4 dyn/cm attributable to this entropy factor.

(12) We are indebted to Professor Ernest Eliel for drawing this to our attention.

Octafluorocyclooctatetraene Transition-Metal Chemistry: 1,2-η and 1,2,3,6-η Complexes of Iron and Platinum

Aldos C. Barefoot, III, Edward W. Corcoran, Jr., Russell P. Hughes,*† David M. Lemal,* and W. Daniel Saunders

Department of Chemistry, Dartmouth College Hanover, New Hampshire 03755

Brian B. Laird and Raymond E. Davis*

Department of Chemistry University of Texas at Austin Austin, Texas 78712

Received September 22, 1980

Cyclooctatetraene (COT)[1] has occupied a prominent place in the historical development of organometallic chemistry.[2] It is a versatile ligand which has exhibited a flexible hapticity in its modes of bonding to transition metals, lanthanides, and actinides.[1,2] Moreover, the elucidation of the nature of metallotropic rearrangements in COT complexes, particularly in $Fe(COT)(CO)_3$ (**1**), occupied the attention of many leading research groups for a number of years.[2] Fluorocarbon organometallics have often proved to be more stable thermally and to exhibit different bonding modes from their hydrocarbon analogues.[3] This communication reports examples of 1,2-η complexes of octafluorocyclooctatetraene (OFCOT, **2**)[4] with iron(0) and platinum(0). These undergo intramolecular oxidative addition reactions, with formation of a metal-carbon σ bond, to afford 1,2,3,6-η bonded complexes.

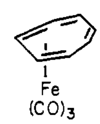

1

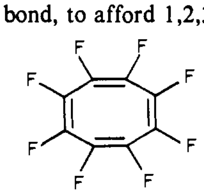

2

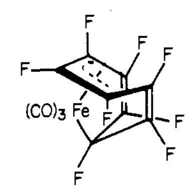

3

Reaction of OFCOT with excess $Fe_2(CO)_9$ in refluxing hexane afforded the pale yellow, sublimable complex **3** as air-stable crystals. The structure of **3** has been established (−30 °C) by single-crystal X-ray diffraction techniques to be that shown in Figure 1.[5]

The coordination geometry around Fe may be described either as (a) trigonal bipyramidal (if the allyl ligand is considered to

† Alfred P. Sloan Research Fellow, 1980–1982.

(1) For a review of cyclooctatetraene and its derivatives, see: Fray, G. I.; Saxton, R. G. "The Chemistry of Cyclooctatetraene and its Derivatives"; Cambridge University Press: Cambridge, 1978.

(2) The organometallic chemistry of cyclooctatetraene is reviewed in ref 1 and in: Deganello, G. "Transition Metal Complexes of Cyclic Polyolefins"; Academic Press: New York, 1979.

(3) Stone, F. G. A. *Pure Appl. Chem.* **1972**, *30*, 551–573.

(4) Lemal, D. M.; Gerace, M. J.; Ertl, H. *J. Am. Chem. Soc.* **1975**, *97*, 5584. Lemal, D. M.; Buzby, J. M.; Barefoot, A. C., III; Grayston, M. W.; Laganis, E. D. *J. Org. Chem.* **1980**, *45*, 3118–3120. Barlow, M. G.; Crawley, M. W.; Haszeldine, R. N. *J. Chem. Soc., Perkin Trans. 1* **1980**, 122.

(5) Complex **3** (38%): mp 126–127.5 °C; ν_{CO}(benzene) 2105, 2060, $\nu_{C=C}$ 1745 cm^{-1}; ^{19}F NMR (1:1 $CDCl_3/C_6H_6$) (chemical shift in ppm upfield from internal $CFCl_3$; relative intensity) δ 113.0 (2 F), 127.9 (3 F), 161.9 (2 F), 170.4 (1 F). Crystals of **3** are orthorhombic, *Pnma*, $a = 10.432$ (2), $b = 13.262$ (2), $c = 8.599$ (2) Å; $Z = 4$. The structure was solved by heavy atom methods and refined by full-matrix least-squares procedures to final agreement factors $R = \sum||F_o| - |F_c||/\sum|F_o| = 0.025$, $R_w = [\sum w(|F_o| - |F_c|)^2/\sum w|F_0|^2]^{1/2} = 0.031$, using 1598 reflections with $I \geq 2.0\sigma(I)$.[6] The molecule is located on the crystallographic mirror plane and thus has rigorous C_s symmetry, with the iron, one carbonyl, the $\sigma\eta$ carbon, and the central carbon of the η^3-allyl carbon, and the central carbon of the η^3-allyl group in the mirror plane. Selected bond lengths (Å): Fe–C1 = 2.078 (1), Fe–C2 = 2.071 (1), Fe–C5 = 2.059 (2), C1–C2 = 1.424 (1), C2–C3 = 1.475 (2), C3–C4 = 1.318 (2), C4–C5 = 1.487 (1). Selected bond angles (deg): C5–Fe–C9 = 177.5 (1), C1–Fe–C5 = 95.7 (1), C1–Fe–C9 = 86.4 (1), C10–Fe–C10′ = 98.4 (1), C10–Fe–C2 = 92.1 (1), C10–Fe–C1 = 130.8 (1), C10–Fe–C2′ = 163.9 (1).

(6) Experimental procedures are essentially as previously delineated: Riley, P. E.; Davis, R. E. *Acta Crystallogr., Sect. B* **1976**, *A32*, 381–386.

0002-7863/81/1503-970$01.25/0

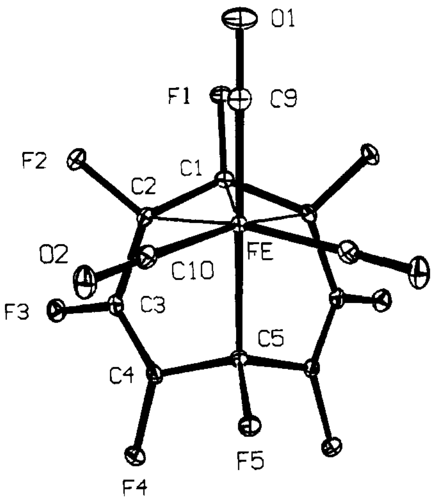

Figure 1. A view of the molecular structure of **3**.[5]

occupy one coordination site) with the ring bridging from an axial site (the σ bond) to an equatorial one (the allyl bond) or as (b) octahedral (considering the allyl to occupy two coordination sites), with the ring bonded in a *fac* manner. The Fe–C(allyl) bond lengths in **3**, term = 2.071 Å, apic = 2.078 Å, are unusually symmetrical compared to other typical reported bonds of this type: term = 2.208 and 2.195 Å, apic = 2.104 Å in allyltricarbonyliron;[7] term = 2.145 and 2.173 Å, apic = 2.038 Å in [6,7,5,9-η:2,3,4,11-η-(11-oxobicyclo[4.3.1]undeca-2,6,8-triene-4,11,-diyl)]bis(tricarbonyliron);[8] term = 2.131 and 2.104 Å, apic = 2.038 Å in [2,3,4,8-η-(9-oxobicyclo[3.2.2]nona-3,5-diene-2,8-diyl)]tricarbonyliron (orthorhombic form);[8] term = 2.195 and 2.317 Å, apic = 2.069 Å in [2,3,4,8-η-(9-oxobicyclo[3.2.2]-nona-3,5-diene-2,8-diyl)]tricarbonyliron (triclinic form);[9] and term = 2.167 and 2.192 Å, apic = 2.089 Å in [1,4,5,6-η-(1-ethoxy-carbonylhexene-1,6-diyl)]tricarbonyliron.[10] This comparison also reveals the unusually short nature of the Fe–C(allyl) bonds in **3**, a result also noted in another highly fluorinated allyliron complex, [2,4-bis(trifluoromethyl)perfluoropenta-2,4-dienyl-cyclopentadienyl](triphenylphosphine)iron,[11] where the bond lengths are term = 1.905 and 1.969 Å, apic = 1.981 Å. Likewise, the Fe–C σ bond in **3**, 2.059 Å, is shorter than typically observed in comparable nonfluorinated complexes, e.g., 2.080 Å in ref 8, 2.110 Å in ref 9, 2.151 Å in ref 10.

The ^{19}F NMR spectrum of **3** (20 °C)[5] demonstrates that the solution structure is identical with that in the solid state and no rapid metallotropic rearrangement is occurring. The bonding of OFCOT to the $Fe(CO)_3$ fragment is considerably different from that of its hydrocarbon analogue (**1**). Comparison of the values of ν_{CO} for **1**[12] and **3**[5] clearly supports the idea that OFCOT undergoes a formal oxidative addition to give **3**. A structural analogue of **3** is not found in the rich iron carbonyl chemistry of the parent cyclooctatetraene but must be sought in osmium chemistry. A complex Os(1,2,3,6-η-COT)$(CO)_3$ is reported to be the kinetic product from the photochemical reaction of COT with $Os_3(CO)_{12}$. This complex readily rearranges on heating to afford the fluxional Os(1-4-η-COT)$(CO)_3$.[13] The two instances in which oxidative addition to produce a 1,2,3,6-η ligand has occurred are internally consistent, for in one, the ligand should have oxidizing character (OFCOT), and in the other, the metal is readily oxidized (osmium).

When the reaction of $Fe_2(CO)_9$ with OFCOT is carried out at 20 °C (hexane or ether) or when photolysis of $Fe(CO)_5$ is carried out in the presence of OFCOT, a second colorless complex is obtained.[14] The infrared spectrum of this complex clearly shows it to be a tetracarbonyliron species. This complex is converted to **3** on heating in hexane, and it releases OFCOT upon treatment with trimethylamine oxide; the most plausible structure seems to be **4**. This represents only the second example of a η^2 complex of a cyclooctatetraene cyclooctatetraene derivative.[15]

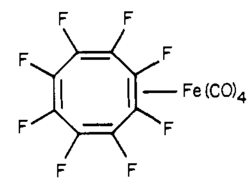

4

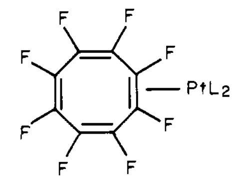

5a, L = PPh_3
b, L = PPh_2Me
c, L = PMe_2Ph

The tendency of OFCOT to undergo oxidative addition reactions is prominent in its chemistry with Pt(0) compounds. Reactions of $Pt(C_2H_4)(PPh_3)_2$, or PtL_4 (L = PPh_3, PPh_2Me, PMe_2Ph), with an equivalent amount of OFCOT (20 °C; C_6D_6, $CDCl_3$) rapidly give the η^2 complexes **5**,[16] which rapidly transform into the 1,2,3,6-η complexes **6** in solution.

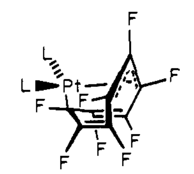

6a, L = PPh_3
b, L = PPh_2Me
c, L = PMe_2Ph

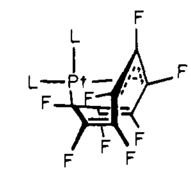

7

Compounds **6** were isolated in quantitative yields as colorless, air-stable crystals.[17] The ^{19}F NMR spectra of **5** and **6** demonstrate rigidity in the Pt–OFCOT bonding at 20 °C. Compounds **6** represent unusual five-coordinate complexes of Pt(II). Two structures were considered for the ground state of these compounds: a tetragonal-pyramidal arrangement around Pt, with the Pt–C σ bond occupying the apical position and the two phosphine ligands occupying symmetrically equivalent basal sites (as in **6**), and a trigonal-bipyramidal arrangement (**7**) with the phosphines occupying symmetrically inequivalent axial and equatorial sites. The ^{31}P{^{1}H} NMR spectrum of **6b**[18] shows only one phosphorus resonance at −100 °C, and the ^{1}H NMR spectrum of **6c** shows two resonances, with ^{195}Pt satellites, for the phosphorus methyl groups.[13] Only a structure (**6**) with symmetrically equivalent

(7) Putnik, C. F; Welter, J. J.; Stucky, G. D.; D'Aniello, M. J., Jr.; Sosinsky, B. A.; Kirner, J. R.; Muetterties, E. L. *J. Am. Chem. Soc.* **1978**, *100*, 4107–4116.

(8) Wang, A. H.-J.; Paul, I. C.; Aumann, R. *J. Organomet. Chem.* **1974**, *69*, 301–304.

(9) Cotton, F. A.; Troup, J. M. *J. Organomet. Chem.* **1974**, *76*, 81–88.

(10) Grevels, F.-W.; Feldhoff, U.; Leitich, J.; Krüger, C. *J. Organomet. Chem.* **1976**, *118*, 79–92.

(11) (a) Nesmayanov, A. N.; Aleksandrov, G. G.; Bokii, N. G.; Zlotina, I. B.; Struchkov, Yu. T.; Kolobova, N. E. *J. Organomet. Chem.* **1976**, *111*, C9–C12. (b) Bokii, N. G.; Kolobova, N. E.; Struchkov, Yu. T. *Koord. Khim.* **1976**, *2*, 278.

(12) Complex **1**: $\nu_{CO}(CS_2)$ 2051, 1992, 1978 cm^{-1}. Manuel, T. A.; Stone, F. G. A. *J. Am. Chem. Soc.* **1960**, *82*, 366–372.

(13) Bruce, M. I.; Cooke, M.; Green, M.; Westlake, D. L. *J. Chem. Soc. A* **1969**, 987–992. Bruce, M. I.; Cooke, M.; Green, M. *Angew. Chem., Int. Ed. Engl.* **1968**, *7*, 639.

(14) Complex **4** (20%): mp 59–63 °C dec; ν_{CO}(hexane) 2125, 2070, 2050, 2030, $\nu_{C=C}$ 1690 cm^{-1}; ^{19}F NMR (acetone-d_6) 97.0 (2 F), 135.3 (4 F), 142.1 (2 F).

(15) Benson et al. (Benson, I. B.; Knox, S. A. R.; Stansfield, R. F. D.; Woodward, P. *J. Chem. Soc., Chem. Commun.* **1977**, 404–405) report the synthesis and structure of Mn(η-C_5H_5)$(CO)_2$(η^2-COT).

(16) **5a**: ^{19}F NMR ($CDCl_3$) δ 115.6 (2 F), 139.1 (2 F, J_{Pt-F} = 256 Hz), 160.2 (2 F), 186.5 (2 F).

(17) Though cyclooctatetraene itself forms platinum(II) complexes (1,2,5,6-η),[1,2] there appears to be no known platinum(0) complex of the parent hydrocarbon.

(18) **6a**: mp 223 °C; $\nu_{C=C}$ 1710, 1720 cm^{-1}; ^{19}F NMR ($CDCl_3$) δ 135.4 (2 F, J_{Pt-F} = 50 Hz), 141.3 (1 F, J_{Pt-F} = 350 Hz), 159.1 (2 F, J_{Pt-F} = 69 Hz), 185.9 (2 F, J_{Pt-F} = 233 Hz), 193.3 (1 F, no observed J_{Pt-F}). Compounds **6b** and **6c** have almost identical ^{19}F NMR spectra.

(19) **6b**: ^{31}P{^{1}H} NMR δ −2.5 (relative to external H_3PO_4) J_{Pt-P} = 2220 Hz; ^{1}H NMR ($CDCl_3$) δ 1.80 (P-*Me*, J_{P-H} = 8.8, J_{Pt-H} = 24.0 Hz). **6c**: ^{1}H NMR ($CDCl_3$) δ 1.55 (P-*Me*, J_{P-H} = 8.8, J_{Pt-H} = 25.5 Hz), 1.49 (P-Me, J_{P-H} = 8.8, J_{Pt-H} = 25.5 Hz).

phosphorus ligands but without a plane of symmetry passing through the Pt–P bond(s) satisfies these observations. Furthermore, rapid equilibration of **6** and **7** via a turnstile or pseudorotation process cannot be occurring at 20 °C.

Octafluorocyclooctatetraene has been shown to be a novel ligand which undergoes oxidative addition reactions with low-valent transition metals. Its coordination chemistry should be as rich as that of its hydrocarbon analogue and is under continuing investigation.

Acknowledgment. Russell P. Hughes acknowledges support from the National Science Foundation (SPI 78-27543) and the donors of the Petroleum Research Fund, administered by the American Chemical Society. We are grateful to Professor John Powell (Toronto) for obtaining the low-temperature $^{31}P\{^1H\}$ spectra. David M. Lemal thanks Mr. Howard S. Hutchins for assistance with ^{19}F NMR and both the National Science Foundation and the donors of the Petroleum Research Fund, administered by the American Chemical Society, for generous financial support. The JEOL FX-60Q NMR spectrometer used in this work was purchased with the help of Grant NSF-CHE77-04386. R. E. Davis acknowledges support by the Robert A. Welch Foundation (Grant F-233) and the National Science Foundation (Grant GP-37028) for purchase of the Syntex $P2_1$ diffractometer used in this work.

Supplementary Material Available: Tables of atomic positional and thermal parameters (2 pages). Ordering information is given on any current masthead page.

Mechanism of Proton Transfer from Intramolecularly Hydrogen-Bonded Acids. Differences between Nitrogen-to-Oxygen and Nitrogen-to-Nitrogen Proton Transfer

A. J. Kresge* and M. F. Powell

Department of Chemistry, University of Toronto Scarborough College, West Hill Ontario, Canada M1C 1A4

Received October 31, 1980

We wish to report that, using an isotropic tracer method to measure rates of proton transfer from the intramolecularly hydrogen-bonded conjugate acid of 2,7-dimethoxy-1,8-bis(dimethylamino)naphthalene, we have obtained data which give a sharply curved biphasic Brønsted plot diagnostic of a two-step reaction mechanism; our results also indicate that nitrogen-to-nitrogen proton transfers are intrinsically slower than nitrogen-to-oxygen proton transfers.

It is well-known that incorporation of an acidic hydrogen into an intramolecular hydrogen bond slows its rate of reaction with external bases by several orders of magnitude. This diminished reactivity was originally explained by a two-step reaction mechanism in which the internal hydrogen bond is first broken to give an acid externally hydrogen bonded to solvent; this unstable intermediate then reacts with the proton acceptor in a normal fast reaction, but the rate of the overall process is slowed by the intermediate's low concentration.[1] It was later pointed out, however, that a single-step mechanism, in which the proton is transferred directly out of the intramolecular hydrogen bond, would also give a reduced rate because its transition state would have a tricoordinated hydrogen with an unfavorable nonlinear arrangement of forming and breaking bonds.[2]

A choice between these two alternatives might be made on the basis of the characteristics expected for the second step of the stepwise mechanism: when the proton donor and the proton acceptor are both nitrogen or oxygen species, this step will give a biphasic Brønsted plot of the kind first observed by Eigen for normal acid–base reactions,[1] and it will also show a sharp isotope effect maximum.[3] In normal acid–base reactions these features appear where the pK_a difference between the proton donor and the protonated proton acceptor is zero, and in the present case this is the point at which $\Delta pK' = 0$, where $\Delta pK'$ refers to the pK_a difference for the actual proton-transfer step (eq 1). This point

$$\underbrace{\mathrm{SH} + \mathrm{B} \rightleftharpoons \overbrace{\mathrm{SH'} + \mathrm{B} \rightleftharpoons \mathrm{S} + \mathrm{HB}}^{\Delta pK'}}_{\Delta pK} \qquad (1)$$

will be displaced in the uphill direction from the place where the overall pK_a difference between the intramolecularly hydrogen-bonded acid and the protonated proton acceptor, ΔpK in eq 1, is zero; the magnitude of this displacement is determined by the value of the preequilibrium constant and is in general appreciable.

This complication makes observation of these features characteristic of the two-step mechanism difficult, inasmuch, as standard kinetic techniques, including fast reaction methods, are limited to the region a few pK units to either side of $\Delta pK = 0$. In the latter region the expected behavior of the two-step mechanism is less diagnostic: Brønsted plots will be monophasic and isotope effects will be constant and near unity. Measurements in this region have nevertheless been made; the results suggest reaction by a two-step mechanism in some cases,[4] but point to the simultaneous operation of both mechanisms in others.[5]

We wish to report that we have developed an isotopic tracer method of making measurements in the more diagnostic region near $\Delta pK' = 0$ and the results we have obtained indicate the operation of a two-step reaction mechanism. We prepared the conjugate acid of 2,7-dimethoxy-1,8-bis(dimethylamino)naphthalene[6] (**1**) labeled with tritium in its acidic nitrogen–hydrogen bond and monitored the loss of this label to solvent in a wholly aqueous medium in the presence of basic catalysts (eq 2)

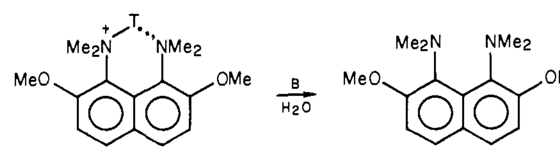

(2)

1

by quenching aliquots of reaction mixture, removing solvent by vacuum evaporation, and subjecting the residues to radioactive assay by liquid scintillation counting. This reaction is strongly uphill and therefore quite reversible at $\Delta pK' = 0$, but the overwhelmingly large pool of hydrogen in the solvent effectively prevents tritium from reentering the substrate.

Kinetic data obtained in this way follow the first-order rate law, as expected. The reaction shows general base catalysis, and standard treatment of the data gives the catalytic coefficients which are displayed in Figure 1 in the form of a Brønsted plot.[7] It may be seen that these rate constants disperse into two categories depending on whether the proton acceptor is an oxygen or a nitrogen base. The oxygen bases give a decidedly biphasic plot

(1) Eigen, M. *Angew. Chem., Int. Ed. Engl.* **1964**, *3*, 1–19.
(2) Haslam, J. L.; Eyring, E. M. *J. Phys. Chem.* **1967**, *71*, 4470–4475 and references cited therein. Fueno, T.; Kajimoto, O.; Nishigaki, Y.; Yosioka, T. *J. Chem. Soc., Perkin Trans. 2* **1973**, 738–741.
(3) Bergman, N. A.; Chiang, Y.; Kresge, A. J. *J. Am. Chem. Soc.* **1978**, *100*, 5954–5956. Cox, M. M.; Jencks, W. P. *Ibid.* **1978**, *100*, 5956–5957.
(4) (a) Hibbert, F.; Awwal, A. *J. Chem. Soc., Chem. Commun.* **1976**, 995–997; *J. Chem. Soc., Perkin Trans. 2* **1978**, 939–945. Awwal, A.; Hibbert, F. *Ibid.* **1977**, 152–156. (b) Hibbert, F.; Robbins, H. J. *J. Am. Chem. Soc.* **1978**, *100*, 8239–8244; *J. Chem. Soc., Chem. Commun.* **1980**, 141–142.
(5) Permutter-Hayman, B.; Shinar, R. *Int. J. Chem. Kinetics*, **1975**, *7*, 453–462, 798. Permutter-Hayman, B.; Sarfaty, R.; Shinar, R. *Ibid.* **1976**, *8*, 741–751. Permutter-Hayman, B.; Shinar, R. *Ibid.* **1977**, *9*, 1–12; **1978**, *10*, 407–415.
(6) Alder, R. W.; Goode, N. C.; Miller, N.; Hibbert, F.; Hunte, K. P. P.; Robbins, H. J. *J. chem. Soc., Chem. Commun.* **1978**, 89–90.
(7) General base catalytic coefficients were determined in buffer solutions at constant ionic strength (0.10 M). Buffer ratios were generally in the range 0.5–2, and base concentrations were usually varied by a factor of 5; this gave general-base contributions to overall reaction rates which ranged from 1.2 to 4 times rates produced by solvent and solvent-related species.

0002-7863/81/1503-972$01.25/0